JOURNAL OF SOLID STATE CHEMISTRY 50, 163–172 (1983)

Bronzes with a Tunnel Structure $K_xP_4O_8(WO_3)_{2m}$: The Tenth Member of the Series—$KP_8W_{40}O_{136}$

PH. LABBÉ, D. OUACHÉE, M. GOREAUD, AND B. RAVEAU

Laboratoire de Cristallographie, Chimie, et Physique du Solide, L.A. 251, Université de Caen, 14032 Caen Cedex, France

Received April 8, 1983; in revised form July 6, 1983

The crystal structure of $KP_8W_{40}O_{136}$, the tenth member of the series $K_xP_4O_8(WO_3)_{2m}$, has been resolved by three-dimensional single-crystal X-ray analysis. The space group is $P2_1/c$ and the cell parameters are $a = 19.589(3)$ Å, $b = 7.5362(4)$ Å, $c = 16.970(3)$ Å and $\beta = 91.864(14)°$. The framework is built up from ReO_3-type slabs connected through pyrophosphate groups. The structure is compared to those of the other members of the series: although the ReO_3-type slabs show a different type of tilting of the WO_6 octahedra, the dispersion of W–O distances is always higher for the octahedra linked to one or two P_2O_7 groups and decreases in proportion as W is farther from these groups. The perovskite cages of the slabs are described and compared to those encountered in the structures of WO_3 and of the bronzes A_xWO_3.

Introduction

Several members of the ternary nonstoichiometric tungsten oxide family $A_xP_8W_{8n}O_{24n+16}$ (A = Rb, K), called monoclinic diphosphate tungsten bronzes, have been synthesized and studied both structurally (*1–4*) and for their electrical properties (*5*). These compounds, whose formulae can also written as $A_xP_4O_8(WO_3)_{2m}$, may be regarded as juxtapositions of ReO_3-type slabs built up of corner-sharing WO_6 octahedra and slices consisting of P_2O_7 groups delimiting hexagonal tunnels in which the A cation is located. The presence of this cation implies that the W atoms possess a mixed valence less than 6. Consequently, these materials reveal metallic properties, which can be interpreted with the bonding model proposed by Goodenough (*6*) for bronze structures.

The X-ray structural investigation of the members with m = 4, 6, 7, and 8 of the series $A_xP_4O_8(WO_3)_{2m}$ shows that the width of a WO_3 slab is directly related to the value of m. In a given structure, the slabs, all of which possess the same width, are built up of parallel chains m WO_6 octahedra long. The compounds with extreme values of m have been considered: crystals with $m = 3$ exist but have a different structure (*7*); crystals with $m > 10$ contain complicated intergrowths as proved by a recent electron microscopy study (*8*). The present paper deals with the member $m = 10$ of the series the highest value of m which can be reasonably investigated by means of X rays.

Experimental

Sample Preparation

Mixtures of $(NH_4)_2HPO_4$, K_2CO_3, and WO_3 in appropriate ratios are first heated in air at 1173 K in a platinum crucible to decompose the phosphate and the carbonate.

0022-4596/83 $3.00

The resultant products are mixed with the suitable amount of metallic tungsten and heated for 10 to 15 days at 1373 K in evacuated silica ampoules, then slowly cooled for 2 days or quenched in air. The final product is a dark-blue powder containing plate or needle shaped crystals.

Determination of the Mean Structure

The crystal selected for the structure determination was a [010] axis needle limited by {100}, {010}, and {001} forms with the dimensions 14 × 90 × 262 μm. The Laue patterns showed a monoclinic symmetry. Weissenberg films gave parameter values in agreement with the powder work results (*9*). The only systematic absences were *h0l* ($l = 2n + 1$) and lead to the space groups *Pc* or *P2/c*. No superstructure reflections were observed.

The intensity of 6752 independent reflections were measured in the θ range 2–40° with a Enraf–Nonius CAD 4 diffractometer, using Mo$K\alpha$ radiation ($\lambda = 0.71069$ Å). The parameters of the data collection such as ω scan (1.10–1.39°), speed of the ω motor relative to the θ one (Type = 5), and counter slit aperture (1.05–1.90 mm) were fixed after a profile analysis of three reflections. The background was measured on each side of the peak and periodic controls verified the stability of the crystal. A least-squares calculation confirmed the values of the lattice parameters: $a = 19.589(3)$ Å, $b = 3.7681(2)$ Å, $c = 16.970(3)$ Å, and $\beta = 91.864(14)°$. Only the 3740 reflections having $\sigma(I)/I \leq 0.333$ were corrected for the Lorentz and polarization effects, and for absorption using a program based on the crystal morphology. The extreme values of the transmission factors were 0.057 and 0.181 ($\mu = 483.9$ cm^{-1}).

The mean structure was solved by the heavy-atom method in the space group *P2/c*. Contrary to the other members of the series, W atoms do not refine if a center of symmetry is placed in the middle of a hexagonal tunnel, but the least-squares refinement converged correctly if a center is fixed in a rhombic tunnel between two hexagonal tunnels along **c** (Fig. 1). The P, K, and O positions were located in the subsequent difference synthesis. Maps of electron density, drawn around each of these atoms, revealed a splitting in (010) for O(13), O(14), O(15), O(16), and O(17) and a splitting parallel to [010] for O(1), O(3), O(4), O(6), O(9), and O(11). In the last refinements, these O atoms were distributed over two neighboring positions with an occupancy factor 0.5. The other atoms seem not to be disordered. Scattering factors for W^{6+}, K^+, and P were from the data of Cromer and Waber (*10*) corrected for anomalous dispersion (*11*) and for O^{2-} from Suzuki (*12*). A linear weighting scheme was adjusted according to $\langle\sqrt{w}||F_o| - |F_c||\rangle$ in terms of $\sin\theta/\lambda$. The results (Tables I and II) lead to values of the conventional $R = 0.040$ and $R_w = 0.049$. A projection (Fig. 1) of the atomic positions onto (010) includes an additional peak *T*, about $2e^-$ high, near O(18), found in the final difference synthesis and discussed later.

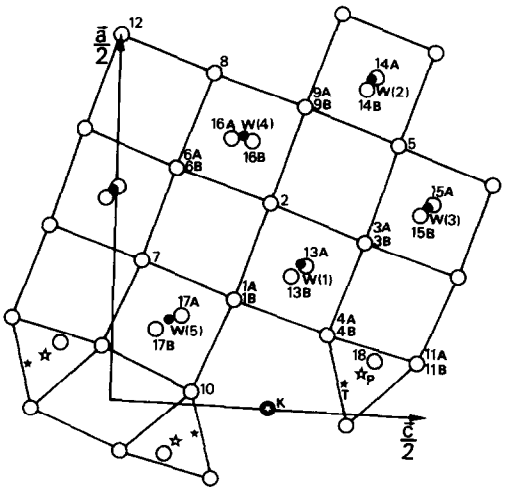

FIG. 1. Projection onto (010) of the mean structure.

TABLE I

POSITIONAL PARAMETERS AND e.s.d.'s
($B_{eq} = \frac{4}{3}\sum_i\sum_j \beta_{ij} a_i a_j$)

	Occupation	x	y	z	B
W(1)	1	0.19986(3)	0.4614(3)	0.29495(4)	B_{eq} 0.21(1)
W(2)	1	0.45919(5)	0.4866(2)	0.39891(5)	B_{eq} 0.30(1)
W(3)	1	0.28959(4)	0.5366(3)	0.49615(4)	B_{eq} 0.23(1)
W(4)	1	0.37252(4)	0.5188(3)	0.19903(4)	B_{eq} 0.27(1)
W(5)	1	0.11661(3)	0.5449(3)	0.09010(4)	B_{eq} 0.22(1)
K	0.25	0.0	0.0070(6)	0.25	2.05(24)
P(A)	0.50	0.0554(5)	0.396(3)	0.3980(6)	0.41(11)
P(B)	0.50	0.0542(5)	0.600(3)	0.3979(6)	0.42(11)
O(1A)	0.50	0.147(1)	0.460(11)	0.190(2)	0.19(29)
O(1B)	0.50	0.139(2)	0.582(13)	0.192(2)	1.13(52)
O(2)	1	0.2779(9)	0.472(6)	0.2444(9)	0.91(22)
O(3A)	0.50	0.231(2)	0.435(11)	0.393(2)	0.40(34)
O(3B)	0.50	0.237(2)	0.581(12)	0.393(2)	0.79(46)
O(4A)	0.50	0.102(1)	0.425(7)	0.338(1)	−0.05(24)
O(4B)	0.50	0.105(2)	0.585(12)	0.340(2)	1.20(49)
O(5)	1	0.3691(9)	0.501(5)	0.446(1)	1.06(26)
O(6A)	0.50	0.325(1)	0.444(8)	0.095(1)	−0.32(23)
O(6B)	0.50	0.328(3)	0.589(14)	0.093(3)	1.50(67)
O(7)	1	0.1968(9)	0.490(6)	0.045(1)	1.03(23)
O(8)	1	0.4553(8)	0.474(5)	0.1505(9)	0.72(20)
O(9A)	0.50	0.411(1)	0.444(8)	0.298(1)	−0.21(25)
O(9B)	0.50	0.411(2)	0.596(15)	0.298(3)	1.71(70)
O(10)	1	0.0177(8)	0.480(5)	0.1263(9)	0.86(19)
O(11A)	0.50	0.075(2)	0.400(10)	0.478(2)	1.06(46)
O(11B)	0.50	0.070(2)	0.580(9)	0.481(2)	0.46(33)
O(12)	0.50	0.5	0.5	0.0	1.09(35)
O(13A)	0.50	0.196(2)	−0.005(14)	0.303(3)	1.46(60)
O(13B)	0.50	0.180(2)	−0.003(11)	0.278(2)	0.88(43)
O(14A)	0.50	0.463(1)	−0.001(8)	0.406(2)	0.09(31)
O(14B)	0.50	0.449(2)	−0.010(15)	0.388(3)	1.22(55)
O(15A)	0.50	0.283(2)	0.007(10)	0.505(2)	0.58(40)
O(15B)	0.50	0.278(2)	0.003(9)	0.477(2)	0.47(36)
O(16A)	0.50	0.366(2)	0.002(13)	0.182(2)	1.06(51)
O(16B)	0.50	0.367(2)	0.005(13)	0.210(3)	1.29(54)
O(17A)	0.50	0.120(2)	0.009(10)	0.098(2)	0.91(44)
O(17B)	0.50	0.096(2)	0.017(11)	0.078(2)	0.84(41)
O(18)	0.25	0.070(5)	−0.010(32)	0.413(6)	2.20(13)
T	0.25	0.050(3)	−0.017(17)	0.366(3)	0.48(62)

Description of the Structure

As mentioned in previous papers (*1–3*) for the members of the family $Rb_xP_4O_8(WO_3)_{2m}$ with $m < 10$, the structure of $K_xP_8W_{40}O_{136}$ can only be described when the *b* parameter is doubled (2 × 3.77 Å). However, the superstructure reflections cannot be observed with X rays because the values of their intensities are too small, but they are visible on electron diffraction patterns, involving the space group $P2_1/c$ in the super cell (*a*, 2*b*, *c*). Thus the occupancy factor ½ of the P positions and the splitting of some oxygen atom peaks can be readily understood in the determination of the mean structure. The atoms for which no splitting is observed, as the five W, O(2), O(5), O(7), O(8), O(10), and O(12) repeat themselves within the structure through the translation **b** (3.77 Å) of the sublattice. The two P atoms have no equivalent translation through **b** in the actual structure and so are allocated occupancy factor ½. The apparently split oxygen atoms are due to positions which are not produced through **b** translations. They correspond to tilted octahedra in the proposed model (Fig. 2) which agrees with the $P2_1/c$ group and yields suitable interatomic distances. There are 10 crystallographically independent WO_6 octahedra, which can be regarded as a chain in the [205] direction (Fig. 3). All the octahedra are well defined except $W(1)O_6$ for which the choice of the pair O(4A)–O(4B) deduced from the mean structure is not unequivocal, leading to approximately the same O–O distances. Two [205] chains (Fig. 3) superposed along [010] are bound, at their ends, by a P_2O_7 group which also links lateral [205] chains through O(4A), O(4B), and O(10). Since O(18) bridges the PO_4 tetrahedra, the *y* values of O(4A) and O(4B) are imposed from classical values of O–O distances. The position of the symmetry centers can be considered either at $y = \frac{1}{4}$ and $\frac{3}{4}$, the mean level of W atoms, or at 0 and ½. Though the first position cannot be completely excluded, the second lead to a more satisfactory host lattice as shown in Fig. 3a.

This framework shows, as for the compound $m = 8$, several empty cavities: *A*, *B*, *B′*, *C*, and *C′* (Figs. 2 and 4) and the *S* cage where K is located. All the *A* cages are not strictly identical because of small local deformations. They are similar to perovskite cages and are defined by 12 O atoms from 8 WO_6 octahedra. The *B* cages are also defined by 12 O atoms belonging to 6 WO_6

TABLE II

INTERATOMIC DISTANCES (Å)

W(1)–O(1A)	2.03(3)	W(1*)–O(1B)	2.13(4)	K–O(1A)	3.70(3)
–O(2)	1.78(2)	–O(2)	1.78(2)	–O(1A)	3.52(3)
–O(3B)	1.85(4)	–O(3A)	1.76(3)	–O(1B)	3.65(5)
–O(4A)	2.08(2)	–O(4B)	2.08(4)	–O(1B)	3.34(5)
–O(13A)	1.76(5)	–O(13A)	2.02(5)	–O(4A)	3.29(3)
–O(13B)	2.07(4)	–O(13B)	1.81(4)	–O(4A)	2.92(3)
				–O(4B)	3.33(4)
W(2)–O(5)	1.96(2)	W(2*)–O(5)	1.96(2)	–O(4B)	2.97(4)
–O(8)	1.90(2)	–O(8)	1.90(2)	–O(10)	2.92(2)
–O(9A)	1.93(2)	–O(9B)	1.97(5)	–O(10)	2.79(2)
–O(12)	1.87(0)	–O(12)	1.87(0)	–O(10)	2.79(2)
–O(14A)	1.84(3)	–O(14A)	1.94(3)	–O(10)	2.92(2)
–O(14B)	1.92(6)	–O(14B)	1.89(6)	–O(13A)	3.91(4)
				–O(13B)	3.55(4)
W(3)–O(3B)	2.01(3)	W(3*)–O(3A)	2.10(3)	–O(17A)	3.54(3)
–O(5)	1.80(2)	–O(5)	1.80(2)	–O(17B)	3.54(3)
–O(6B)	1.85(5)	–O(6A)	1.80(2)	–O(18)	3.04(10)
–O(7)	2.02(2)	–O(7)	2.02(2)		
–O(15A)	1.78(4)	–O(15A)	2.01(4)	P(B)–O(4A)	1.55(2)
–O(15B)	2.05(3)	–O(15B)	1.80(3)	–O(10)	1.52(2)
				–O(11A)	1.59(4)
W(4)–O(2)	2.04(2)	W(4*)–O(2)	2.04(2)	–O(18)	1.52(9)
–O(6B)	1.99(5)	–O(6A)	1.99(2)		
–O(8)	1.85(2)	–O(8)	1.85(2)	P(A)–O(4B)	1.58(4)
–O(9A)	1.84(2)	–O(9B)	1.84(5)	–O(10)	1.53(2)
–O(16A)	1.97(5)	–O(16A)	1.85(5)	–O(11B)	1.59(3)
O(16B)	1.84(5)	–O(16B)	1.95(5)	–O(18)	1.58(9)
W(5)–O(1A)	1.81(3)	W(5*)–O(1B)	1.78(3)		
–O(7)	1.78(2)	–O(7)	1.78(2)		
–O(10)	2.06(2)	–O(10)	2.07(2)		
–O(11A)	2.06(3)	–O(11B)	2.09(4)		
–O(17A)	1.75(4)	–O(17A)	2.02(4)		
–O(17B)	2.04(4)	–O(17B)	1.83(4)		

Note. The W atoms with * have $0.5 < y < 1$ in the actual structure.

octahedra and 1 P_2O_7 group. The *B* and *B'* cages, whose repetition along [010] is closely related to the superstructure, are, respectively, limited by 12 and 11 O atoms, O(18) being absent in the second case. Along the tunnels of the rhombic section, two types of cages *C* and *C'* come together in the [010] direction. Since the position of the center of symmetry in the actual structure is fixed, the P_2O_7 groups which form these tunnels with the $W(5)O_6$ octahedra are at the same level *y* and they build the *C* cages as defined by 12 atoms from four WO_6 octahedra. On each side of a *C* cage along [010], the *C'* cages are bordered by 10 O atoms owing to the fact that the atoms of the bridge P–O–P are missing. The *C* and *C'* cages connect, respectively, with the *B* and *B'* cages and also with the *S* sites.

At the center of a hexagonal tunnel lies a 2_1 axis of the actual structure. Consequently, all the host *S* sites of a tunnel are equivalent (Fig. 2). Their surroundings are the same: four octahedra $W(1)O_6$, four octahedra $W(5)O_6$, and one group P_2O_7. Thus, the *S* site is bordered by 17 atoms. The K^+

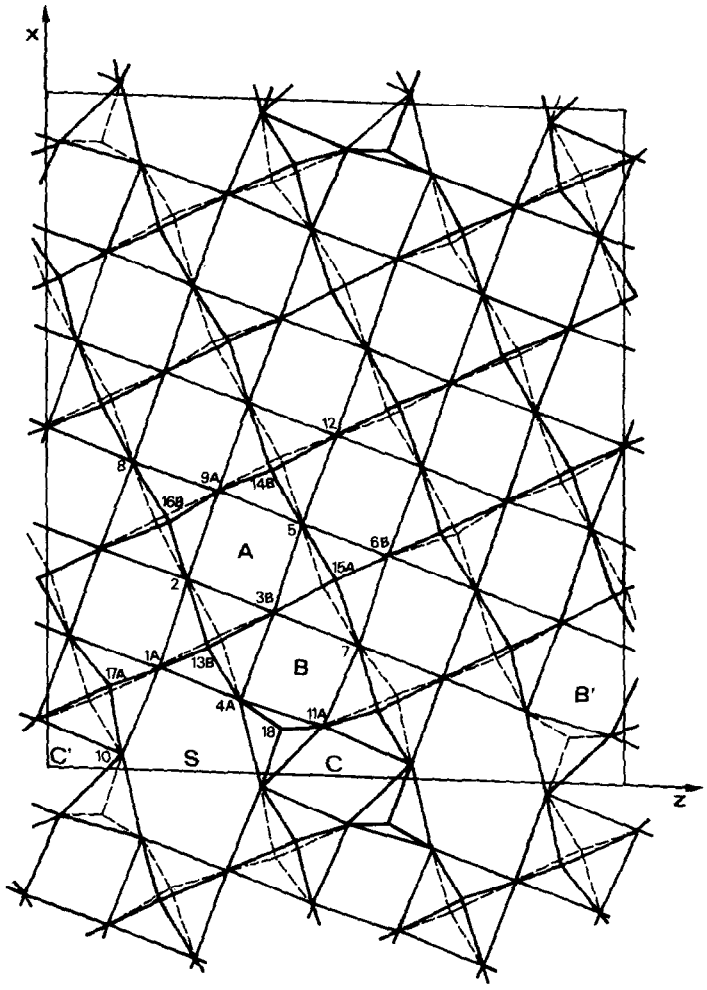

FIG. 2. Projection onto (010) of the actual structure limited to the oxygen framework from $y = 0$ to $y = 0.5$.

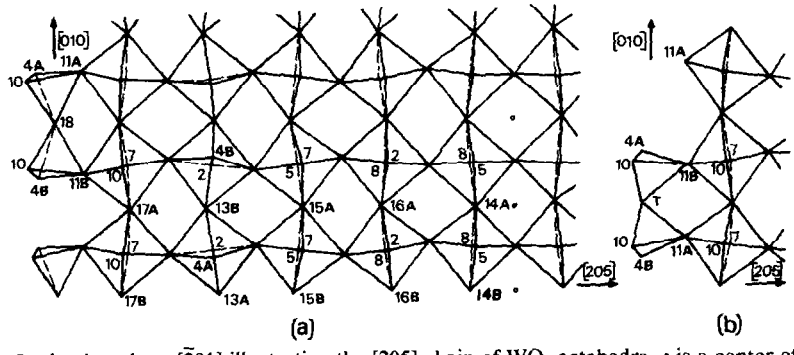

FIG. 3. Projection along $[\bar{2}01]$ illustrating the [205] chain of WO_6 octahedra. ◦ is a center of symmetry. (a) The diphosphate group contains O(18); (b) the diphosphate group contains T.

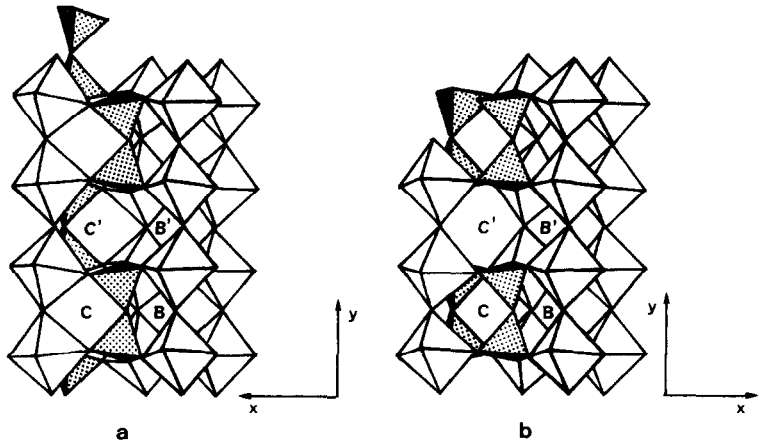

FIG. 4. Cavities B, B', C, and C'. (a) In the phase $n = 4$; (b) in the phase $n = 5$.

ions would be statistically distributed over all the S sites with an occupancy factor 0.25. Table II shows seven short K–O distances 2.79–3.04 Å and three longer distances 3.29–3.34 Å, involving an anisotropic coordination for the K atom probably not similar to that encountered in the hexagonal tungsten bronze structure K_xWO_3 (*13*, *14*). The tetrahedra of the P_2O_7 groups are quite regular with P–O distances ranging from 1.52(2) to 1.59(4) Å (Table II). The O(18) atom of the bridge is, in the (010) projection, displaced towards the O(4)–O(11) edge. It results in a tilting of the P_2O_7 group with P–O(18)–P = 152° which has the same value as that in the other members of the series.

Discussion and Conclusion

The T Peak

The existence of the T peak (Fig. 1) has been verified. In a previous study another crystal from the same preparation was investigated. All the above features such as lattice parameters, position of the origin, and splitting of O atom peaks were the same, but the Fourier difference map showed numerous additional peaks including T. All these peaks, except T, were interpreted as W atoms at the center of octahedra which continue the linear chains of five WO_6 octahedra of the $m = 10$ compound. So, the crystal must contain intergrowths of WO_3 slabs of various widths, most equal to $m = 10$ but a few with $m \neq 10$ as confirmed by means of high resolution electron microscopy (Fig. 5). However, this idea has not been able to explain the presence of the T peak.

The hypothesis that a cation C is located between two P_2O_7 groups leads to distances C–O in the range of 1.91–2.52 Å, distances C–P about 2.34 Å, and very inhomogeneous coordination. The identification of T with a fraction of an oxygen atom as O(18) seems to be more probable: it involves another type of P_2O_7 group which could be placed at a level situated between two previously described P_2O_7 (Fig. 3) and able to replace them. It implies a second possible choice for the pair O(4A)–O(4B). The two tetrahedra would have mean values P–O of 1.51 and 1.54 Å but an angle P–T–P of about 140°. Though it leads to less regular O–O distances (2.30–2.59 Å) than in the first case (2.45–2.65 Å), this hypothesis of a second sort of P_2O_7 group binding the [205] chains practically without any change for

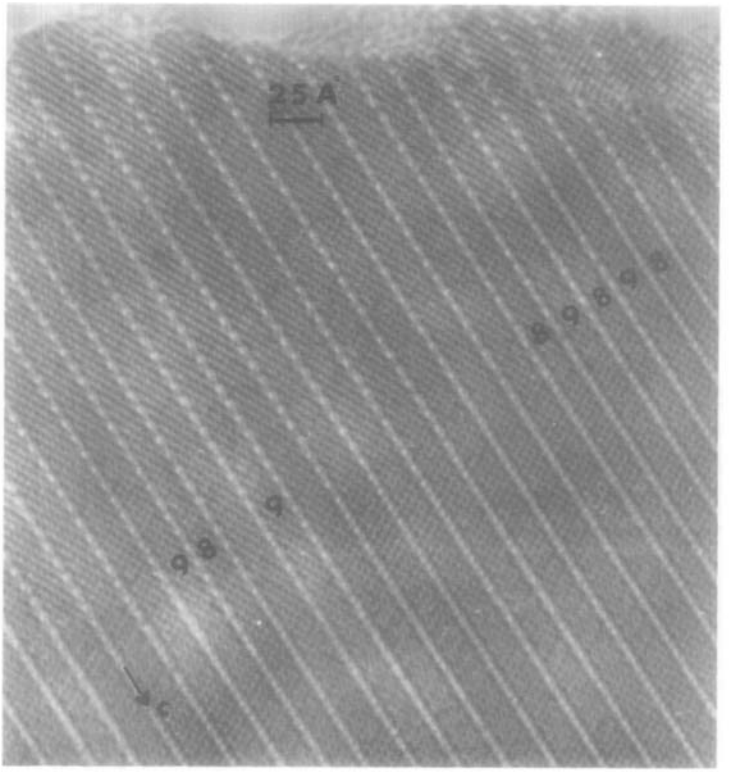

FIG. 5. Micrograph, viewed along **b**, of a crystal fragment with nominal composition $m = 10$ showing disorder: $m = 8$ and $m = 9$ members can be seen in the matrix.

the WO_3 lattice, is attractive because it can explain an electron diffraction observation where, for about 20% of the photographs, $h0l$ reflections with $l = 2n + 1$ are visible, i.e., for which a **c** glide plane, is not strictly consistent with the structure.

The Behavior of the W Atoms

Table III shows the main features of the W positions for the structures we have already studied in the series. It gives, for each octahedron, the W–O distances, the displacement D of W with respect to their mean plane (010), and the distance d between W and the center G of its octahedron. We can observe that the dispersion of W–O distances is systematically highest when they are included in the octahedra linked to one or two P_2O_7 groups and decreases regularly in proportion as W is farther from the P_2O_7 groups. The maximum observed dispersion is 0.40 Å and the minimum, about 0.13 Å, is practically the same for the octahedra located far from the tetrahedra, i.e., the last two lines for each compound (Table III). For these W atoms, the displacements D and d are the weakest involving a greater rigidity of the octahedra situated in the central part of the WO_3 slabs, the deformation and the tilting of the octahedra being more and more important as they approach the diphosphate group.

The ReO_3-type Slabs

As pointed out above, the present cyrstal structure ($m = 10$) differs from those of the other members of the monoclinic family $A_xP_4O_8(WO_3)_{2m}$. According to the new rela-

TABLE III

DISTANCES RELATIVE TO W ATOMS IN THE $A_xP_4O_8(WO_3)_{2m}$ FAMILY

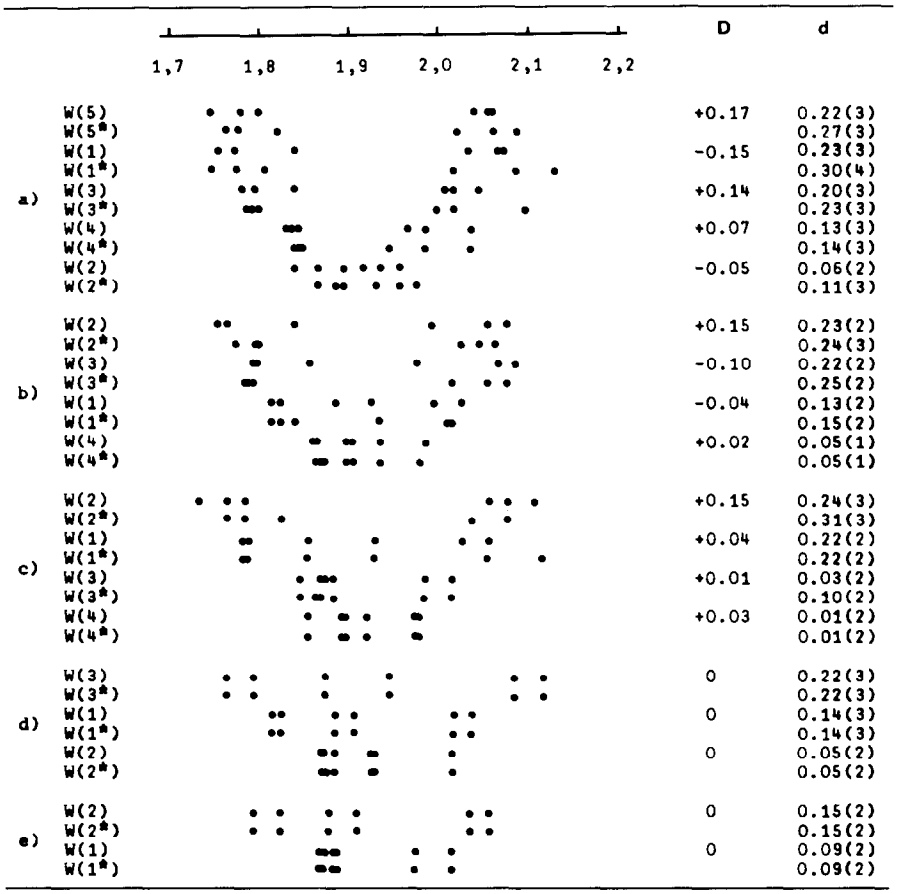

Notes. *D*: displacement (Å) of W with respect to their mean plane (010). *d*: distance (Å) between W and the center *G* of each octahedron. In each graph, the W atoms are arranged according to increasing distances to the P_2O_7 groups. The first two W are in octahedra linked to two tetrahedra, the third and the fourth to one tetrahedron. The W atoms with * have $0.5 < y < 1$. (a) $m = 10$, (b) $m = 8$, (c) $m = 7$, (d) $m = 6$, (e) $m = 4$.

tive disposition of the 2_1 axes and the symmetry centers, the distribution of the W atoms and the P_2O_7 groups gives the $m = 10$ compound its particular features. Indeed, the observed distortion of the ReO_3-type slabs is here quite different from those encountered in the other members of the series. Let us consider, as an example, the $m = 8$ compound (Fig. 6a). The WO_3 host lattice, in the middle part of its slice, is quite regular as ReO_3 and shows a progressive tilted distortion of the octahedra, proportional to their distance from the diphosphate groups. Each octahedron is rotated around a median which joins, in (010), the midpoints of two opposite sides. On the contrary, in the $m = 10$ compound, the octahedra are rotated around one of their diagonals (Fig. 6b) parallel to $[\bar{2}01]$. So, along a [205] chain of 10 WO_6, the octahedra are tilted in a staggered manner and the deformation occurs from one end of the chain to

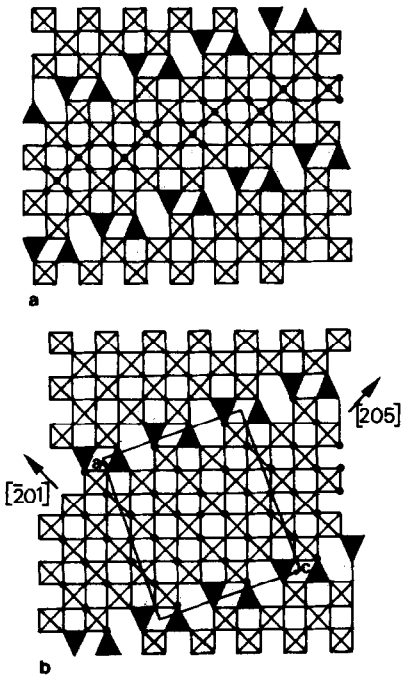

FIG. 6. Projection onto (010) of the idealized structures $A_xP_4O_8(WO_3)_{2m}$. The black points are nonsplit oxygen atoms positioned along [010]. (a) $m = 8$; (b) $m = 10$.

the other, where it is limited by P_2O_7 groups.

It is worthy of note that the shape of the windows which limit the perovskite cages is not the same for the two projections along [010] and [$\bar{2}$01] (Figs. 2 and 3); we indeed observe, respectively, a square (*s*) and a diamond-shaped (*d*) window (Fig. 8) which correspond to the two sorts of windows generally encountered according to the tilting of the octahedra. Furthermore, in the third direction of the perovskite cage, we find again a square-shaped window (Fig. 7). The stacking of these windows may lead to different sorts of perovskite cages owing to the two possible orientations *d* and *d'* of the diamond-shaped window, with respect to one another (Fig. 8). In this respect, the shape of the perovskite cages is to be compared with that observed in ReO_3, in the different WO_3 forms, and in the alkaline bronzes Na_xWO_3 and Li_xWO_3. Along the [010] and [205] directions, we observe only a stacking of square windows which can be described as (*s*, *s*) exactly as for ReO_3 which exhibits such a succession but in the three directions; this (*s*, *s*) succession is also observed in Na_xWO_3 for $x = 0.54$ and 0.73, but with a weak distortion of the perovskite windows (*15*). Along the third direction [$\bar{2}$01], the diamond-shaped windows take alternately two orientations, leading to the sequence (*d*,*d'*) as observed for the monoclinic and triclinic forms of WO_3 (*16, 17*). The shapes of the perovskite cages are, however, different from those observed in WO_3: triclinic WO_3 exhibits indeed a (*d*,*d'*) sequence along the three directions of the structure, whereas monoclinic WO_3 exhibits the sequence (*d*,*d'*) along two directions only, the third direc-

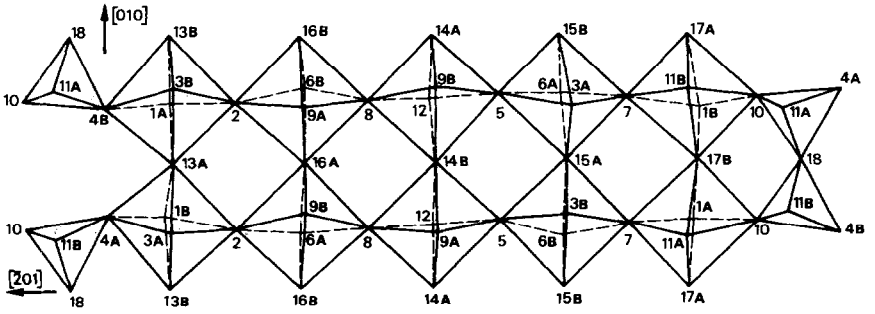

FIG. 7. Projection along [205] showing a chain of WO_6 octahedra parallel to [$\bar{2}$01].

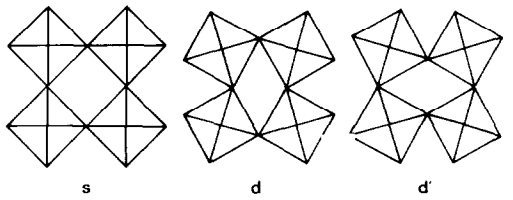

FIG. 8. Shapes of windows encountered in the perovskite cages of ReO_3 and WO_3.

tion corresponding to the sequence (d,d) as also recently observed for the three directions of the structure of $Li_{0.36}WO_3$ (*15*).

The distortion of the WO_3 framework can also easily be observed from the W–O–W angles and the W–O distances along the three directions [010], [$\bar{2}$01], and [205] which characterize the strands of octahedra. Along [010] we indeed observe alternately a high and a smaller value of the W–O–W angle (ranging from 151 to 171°), and of the W–O distances (ranging from 1.76 to 2.06 Å). This is easily explained by the constraint imposed by the P_2O_7 groups: groups of two octahedra are indeed alternately connected to one P_2O_7 group and two P_2O_7 groups. The succession of short and long W–O distances is also found along the [$\bar{2}$01] and [205] directions but the W–O–W angles, although different from 180° (158 to 180°) do not exhibit the same tendency: these angles are almost invariant along [$\bar{2}$01] (172.5 to 175.9°) whereas they range from 153. 5 to 165.6° with an exception in the middle of the slabs (180°) along [205]. This behavior and especially the off-centering of W in its octahedra is very different from that observed in the cubic bronze Na_xWO_3 (*15*) for which a high symmetry of the WO_6 octahedron is always verified. It must finally be pointed out that $KP_8W_{40}O_{136}$ exhibits, like Na_xWO_3, a metallic behavior, but is supposed to exhibit a strong anisotropy owing to the presence of the diphosphate "planes" which connect the WO_3 slabs. In this respect, it would be interesting to correlate the electron transport properties of single crystals of all these bronzes to their structural properties, particularly to the perovskite cage features.

References

1. J. P. GIROULT, M. GOREAUD, PH. LABBÉ, AND B. RAVEAU, *Acta Crystallogr. Sect. B* **36,** 2570 (1980).
2. J. P. GIROULT, M. GOREAUD, PH. LABBÉ, AND B. RAVEAU, *Acta Crystallogr. Sect. B* **37,** 1163 (1981).
3. J. P. GIROULT, M., GOREAUD, PH. LABBÉ, AND B. RAVEAU, *Acta Crystallogr. Sect. B* **38,** 2342 (1982).
4. J. P. GIROULT, M. GOREAUD, PH. LABBÉ, AND B. RAVEAU, *Rev. Chim. Mineral.* to be published.
5. J. P. GIROULT, M. GOREAUD, PH. LABBÉ, J. PROVOST, AND B. RAVEAU, *Mater. Res. Bull.* **16,** 811 (1981).
6. J. B. GOODENOUGH, "Les oxydes des métaux de transition" (Gauthier Villars, Ed.), Paris (1973).
7. B. DOMENGÈS, M. GOREAUD, PH. LABBÉ, AND B. RAVEAU, *Acta Crystallogr. Sect. B* **38,** 1724 (1982).
8. M. HERVIEU AND B. RAVEAU, *Chem. Scr.* **22,** 117 (1983).
9. D. OUACHÉE, Diplôme d'Etudes Approfondies, Caen (1982).
10. D. T. CROMER AND J. T. WABER, *Acta Crystallogr.* **18,** 104 (1965).
11. D. T. CROMER, *Acta Crystallogr.* **18,** 17 (1965).
12. T. SUZUKI, *Acta Crystallogr.* **13,** 279 (1960).
13. L. KIHLBORG AND A. HUSSAIN, *Mater. Res. Bull.* **14,** 667 (1979).
14. M. F. PYE AND P. G. DICKENS, *Mater. Res. Bull.* **14,** 1397 (1979).
15. P. J. WISEMAN AND P. G. DICKENS, *J. Solid State Chem.* **17,** 91 (1976).
16. B. O. LOOPSTRA AND H. M. RIETVELD, *Acta Crystallogr. Sect. B* **25,** 1420 (1969).
17. R. DIEHL, G. BRANDT, AND E. SALJE, *Acta Crystallogr. Sect. B* **34,** 1105 (1978).